

Recent development of NH dynamical core of global IFS

J. Vivoda

with I. Polichtchouk, M. Diamantakis

EWGLAM 2023, 25-28/9/2023



H/NH spectral SISL IFS development/optimization and km-scale research

- NH model improvements enable reliable systematic comparisons
- New gravity wave diagnostics help to assess NH versus H
- new flexible physics-dynamics coupling work in progress opens new prospects
- AMD GPU porting and optimization: successful 4.4km IFS runs on LUMI

IFS finite volume model Gt4Py DSL

- First (single node) global version for IFS grids and unstructured meshes available
- Multi-node CPU/GPU performance study with Gt4Py version 1 (LAM config) published demonstrating near optimal scaling

Basic choice

Existing HY dynamics is an "asymptotic" limit of NH system. NH dynamics must provide exactly the same results for hydrostatic flow regimes as HY dynamics does.

Hydrostatic pressure (mass) coordinate

Laprise, 1992 proposed to use hydrostatic pressure as vertical coordinate. Definition of hydrostatic pressure π is

$$\frac{\partial \phi}{\partial \eta} = - \frac{\partial \pi}{\partial \eta} \frac{RT}{p}$$

HY model

NH model

Vertical coordinate

pressure based hybrid coordinate

$$\pi = A(\eta) + B(\eta)\pi_s$$

$$p = \pi$$

mass based hybrid coordinate (Laprise, 1992)

$$\pi = A(\eta) + B(\eta)\pi_s$$

real pressure (new prognostic quantity)

$$p = \pi e^{\hat{q}}$$

HY model

Grid point space

$$\vec{v} = (u, v), T, q_s = \ln(\pi_s)$$

Spectral space

$$(D, \xi), T, q_s = \ln(\pi_s)$$

NH model

$$\vec{v} = (u, v, gw), T, q_s = \ln(\pi_s), \hat{q} = \ln\left(\frac{p}{\pi}\right)$$

$$(D, \xi, d), T, q_s = \ln(\pi_s), \hat{q}$$

$$d = -\frac{p}{RT} \frac{1}{m} \frac{\partial gw}{\partial \eta} + \frac{p}{RT} \vec{\nabla} \phi \frac{1}{m} \frac{\partial \vec{v}}{\partial \eta}$$

Why d ? \Rightarrow It allows fully implicit treatment of $D3$ term. (stability issues).

For simplicity all equations on my slides are cast on non-rotating cartesian plane (x, y) .

Continuous nonlinear model in η

HY model

Continuity equation

$$\frac{\partial q_s}{\partial t} = -\frac{1}{\pi_s} \int_0^1 \vec{\nabla} \cdot (m\vec{v}) d\eta$$

First law of thermodynamics

$$\frac{dT}{dt} = \frac{\kappa T \omega}{\pi}$$

Horizontal momentum equation

$$\frac{d\vec{v}}{dt} = -\frac{RT}{\pi} \vec{\nabla} \pi - \vec{\nabla} \phi$$

Vertical momentum equation

$$\frac{dg_w}{dt} = \frac{g^2}{m} \frac{\partial(p-\pi)}{\partial \eta}$$

Pressure departure evolution

$$\frac{d\hat{q}}{dt} = -\left(\frac{\omega}{\pi} + \frac{C_p}{C_v} D_3\right)$$

NH model

$$\frac{\partial q_s}{\partial t} = -\frac{1}{\pi_s} \int_0^1 \vec{\nabla} \cdot (m\vec{v}) d\eta$$

$$\frac{dT}{dt} = \frac{\kappa T \omega}{\pi} - \kappa T \left(\frac{\omega}{\pi} + \frac{C_p}{C_v} D_3 \right)$$

$$\frac{d\vec{v}}{dt} = -\frac{RT}{\pi} \vec{\nabla} \pi - RT \vec{\nabla} \hat{q} - \vec{\nabla} \phi - \frac{1}{m} \frac{\partial(p-\pi)}{\partial \eta} \vec{\nabla} \phi$$

SI linear system obtained by traditional linearisation

HY model

NH model

Linear SI system (\mathcal{L})

$$\frac{\partial D}{\partial t} = -RG^* \Delta T - RT^* \Delta q_s - \Delta \phi_s$$

$$\frac{\partial T}{\partial t} = -\kappa T^* \mathbf{S}^* D$$

$$\frac{\partial q_s}{\partial t} = -\mathbf{N}^* D$$

$$\frac{\partial D}{\partial t} = -RG^* \Delta T + RT^* (\mathbf{G}^* - 1) \Delta \hat{q} - RT^* \Delta q_s - \Delta \phi_s$$

$$\frac{\partial T}{\partial t} = -\kappa T^* \mathbf{S}^* D$$

$$+ \kappa T^* \left(\mathbf{S}^* D - \frac{c_p}{c_v} (D + d_4) \right)$$

$$\frac{\partial q_s}{\partial t} = -\mathbf{N}^* D$$

$$\frac{\partial d_4}{\partial t} = -\frac{g^2}{RT_a^*} \mathbf{L}^* \hat{q}$$

$$\frac{\partial \hat{q}}{\partial t} = \mathbf{S}^* D - \frac{c_p}{c_v} (D + d_4)$$

We define vertical operators

$$\begin{array}{l} \mathbf{G}^* X = \int_{\eta}^1 \frac{m^*}{\pi^*} X d\eta \\ \mathbf{N}^* X = \frac{1}{\pi_s^*} \int_0^1 m^* X d\eta \end{array} \quad \left| \quad \begin{array}{l} \mathbf{S}^* X = \frac{1}{\pi^*} \int_0^{\eta} m^* X d\eta \\ \mathbf{L}^* X = \frac{\pi^*}{m^*} \frac{\partial}{\partial \eta} \left(\frac{\pi^*}{m^*} \frac{\partial}{\partial \eta} + 1 \right) X \end{array} \right.$$

Implicit solution for 2TL schemes

Voitus published recently (Degrauwe et al, 2020) that NH spectral solver can be solved for horizontal divergence D . This allows to make HY and NH spectral computations compatible.

HY model

NH model

SI spectral solver

$$[I - \delta t^2 B \Delta] D = RHS_D$$

$$B = RT^* (\kappa \mathbf{G}^* \mathbf{S}^* + \mathbf{N}^*)$$

$$[1 - \delta t^2 B \Delta] D = RHS_D$$

$$B = RT^* [\kappa \mathbf{G}^* \mathbf{S}^* + \mathbf{N}^*] + c^{*2} B_{NH}$$

Single precision problem

B eigenvalues must be all real and positive. This ensures all solutions of \mathcal{L} are constant amplitude waves. This was not satisfied \Rightarrow problem in B_{NH} .

NH SI spectral solver CY47R3

$$B_{NH} = c^{*2} \left(I - \frac{C_v}{C_p} \mathbf{S}^* \right) \left(I + \delta t^2 c^{*2} \mathbf{H}_v^{*-1} \frac{\mathbf{L}^*}{rH^{*2}} \right) \left(I - \frac{C_v}{C_p} \mathbf{G}^* \right) \quad \text{wrong eigenvalues of B}$$

with $\mathbf{H}_v^* = \left(I - \delta t^2 c^{*2} \frac{\mathbf{L}^*}{rH^{*2}} \right)$.

NH SI spectral solver simplification

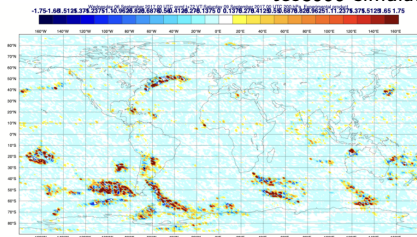
$$B_{NH} = c^{*2} \left(I - \frac{C_v}{C_p} \mathbf{S}^* \right) \left(\underbrace{I - \mathbf{H}_v^{*-1} \mathbf{H}_v^*}_{\text{never 0 on computer}} + \mathbf{H}_v^{*-1} \right) \left(I - \frac{C_v}{C_p} \mathbf{G}^* \right)$$

⇓

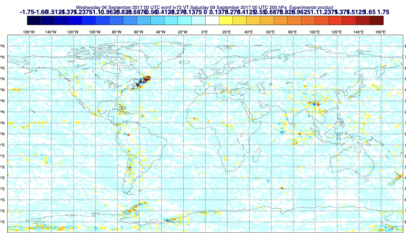
$$B_{NH} = c^{*2} \left(I - \frac{C_v}{C_p} \mathbf{S}^* \right) \mathbf{H}_v^{*-1} \left(I - \frac{C_v}{C_p} \mathbf{G}^* \right) \quad \text{correct eigenvalue of B}$$

VFE discretisation - instabilities in model forecast

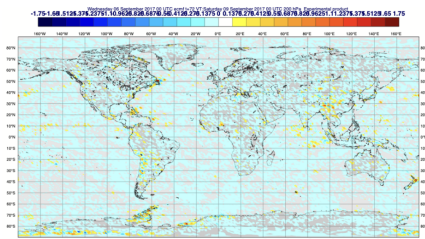
tco3999 simulation w at 200hPa



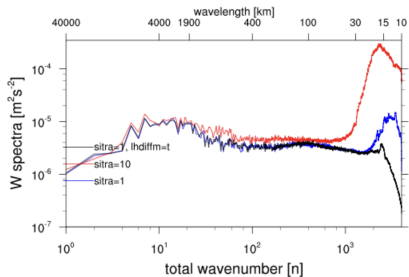
(a) Tco3999 NH-IFS, SITRA=10.



(b) Tco3999 NH-IFS, SITRA=1.



(c) Tco3999 NH-IFS, SITRA=1, old (stronger) diffu-



(d) Tco3999 NH-IFS, w-spectra.

Nonlinear model

\mathbf{L}^* not explicitly in system, combination of RHS of g_w + transformation into d

$$\begin{aligned} \frac{dg_w}{dt} &= \frac{g^2}{m} \frac{\partial p - \pi}{\partial \eta} \approx \frac{g^2}{m} \mathbf{D}_{\text{FH}} \cdot (p - \pi) \\ d &= -\frac{p}{RT} \frac{1}{m} \frac{\partial g_w}{\partial \eta} + \dots \approx -\frac{p}{RT} \frac{1}{m} \mathbf{T}_{\text{HF}} \cdot g_w + \dots \end{aligned} \quad (1)$$

Linear model

\mathbf{L}^* explicitly in system on RHS of d equation

$$\begin{aligned} \frac{\partial d_4}{\partial t} &= -\frac{g^2}{RT_a^*} \mathbf{L}^* \hat{q} = -\frac{g^2}{RT_a^*} \left[\frac{1}{m^*} \frac{\partial}{\partial \eta} \left(\frac{\pi^{*2}}{m^*} \right) \frac{\partial \hat{q}}{\partial \eta} + \left(\frac{\pi^*}{m^*} \right)^2 \frac{\partial^2 \hat{q}}{\partial \eta^2} \right] \\ &\approx -\frac{g^2}{RT_a^*} \left[\frac{1}{m^*_l} \left(\mathbf{D}_1 \frac{\pi^{*2}}{m^*} \right) (\mathbf{D}_2 \hat{q}) + \left(\frac{\pi^*}{m^*} \right)_l^2 (\mathbf{D}\mathbf{D}\hat{q}) \right] \end{aligned}$$

reformulated as

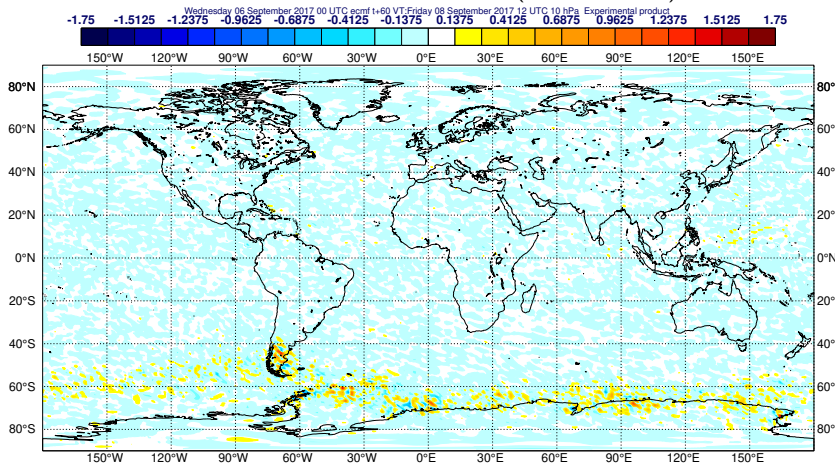
$$\approx -\frac{g^2}{RT_a^*} \left[\frac{1}{m^*_l} \mathbf{T}_{\text{HF}} \cdot \left(\frac{1}{m^*_l} \mathbf{D}_{\text{FH}} \hat{q} \right) \right]. \quad (2)$$

Mandatory BBC is $\left(\frac{\partial p - \pi}{\partial \eta} \right)_s = 0$, in discretized form $(\mathbf{D}_{\text{FH}} X)_s = 0$ at model surface. This ensures all eigenvalues of \mathbf{L}^* to be real and negative.

VFE with consistent of vertical laplacian term L^*

This allows usage of $T_a^* = 100K$ in VFE simulation with NH model. NH simulations are noise free.

NH tco3999 simulation w at 200hPa (new VFE of L^*)



2TL scheme with hybrid coordinate becomes unstable in the presence of high orography

As mountain peaks reach altitude above 8500m, the surface pressure is approaching "monotonicity" limit of hybrid coordinate. The SI scheme is no more capable to handle instabilities related to residuals related to difference between actual surface pressure π_s and reference surface pressure π_s^*

When $\sigma = \frac{\pi}{\pi_s}$ coordinate is used then stability of 2TL scheme doesn't depend on the choice of π_s^* . When hybrid coordinate $\pi = A(\eta) + B(\eta)\pi_s$ with $A(\eta) > 0$ is used, then there always exists minimum surface pressure π_m for which $\frac{\partial \pi}{\partial \eta} \leq 0$ and monotonicity of coordinate is broken (in current oper 137 levels $p_m = 303hPa$).

Stability analysis suggests that 2TL scheme with $T^* = 300K$, $T_a^* = 100K$ is stable as surface pressure satisfies $\alpha\pi_m \leq \pi_s \leq \pi_s^*$ (with $\alpha \in (1.5, 2)$ - empirical values)

NH dynamics - stabilisation with smaller T_a^*

π_s^* related stability for $\pi_s^* = 1000hPa$, $T^* = 300K$ and hybrid coord with $\pi_m = 303hPa$

Figure: $T_a^* = 100K$, PC unstable for $\pi_s < 450hPa$

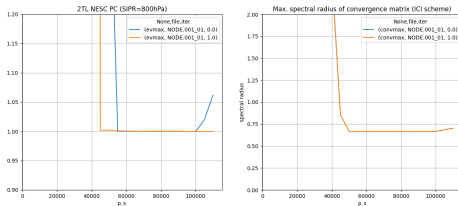
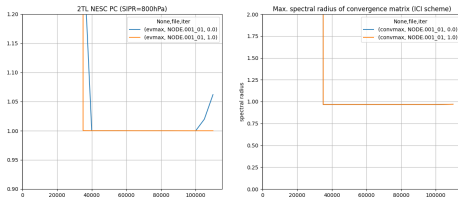


Figure: $T_a^* = 10K$, converge of ICI scheme toward Crank-Nicholson solution is lost



NH dynamics - stabilisation new coordinate definition with smaller π_m

π_s^* related stability for $\pi_s^* = 1000hPa$, $T^* = 300K$ and $T_a^* = 100K$

Figure: $\pi_m = 149hPa$, unstable for $\pi_s < 300hPa$

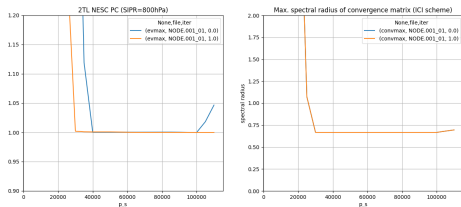
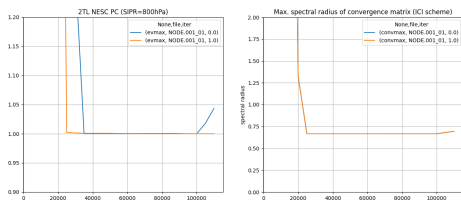
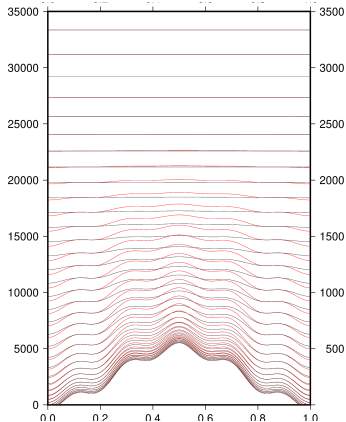


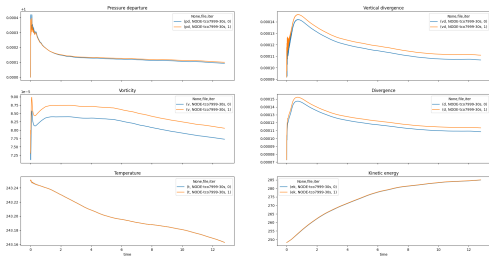
Figure: $\pi_m = 119hPa$, unstable for $\pi_s < 250hPa$



Oper vertical levels with $p_m = 303hPa$ (black) and new levels with $p_m = 149hPa$ (red)



First stable 12h integration with IFS NH run - tco7999 (1.3km). Evolution of norms. Strong initial shock visible - initialisation needed (future plan)

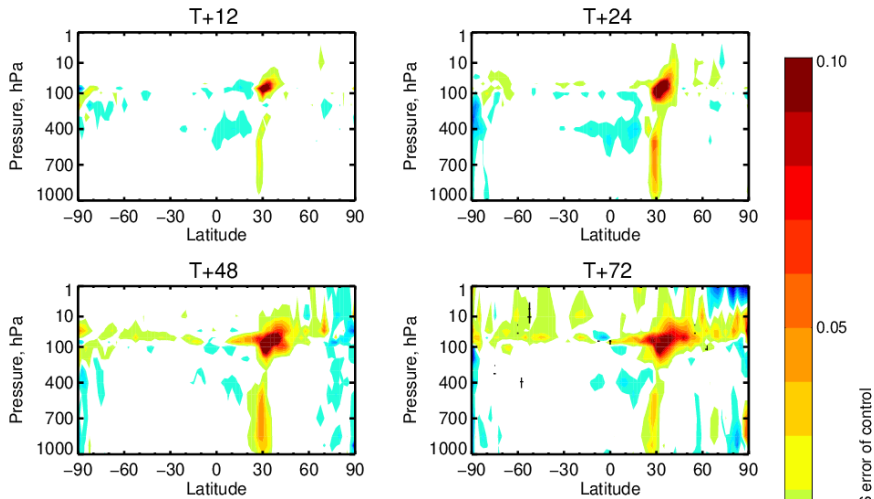


A and B with smaller π_m - effect on score at oper resolution

Change in RMS error in VW (ABs psmono 230hPa psref 400hPa (hw7c)-tco1279 adiabatic (hw4y))

20-Jan-2022 to 24-Jan-2022 from 0 to 5 samples. Verified against 0001.

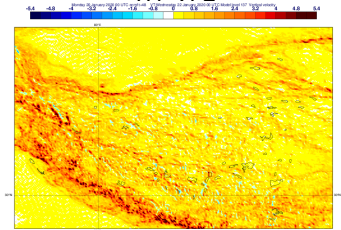
Cross-hatching indicates 95% confidence with Sidak correction for 20 independent tests.



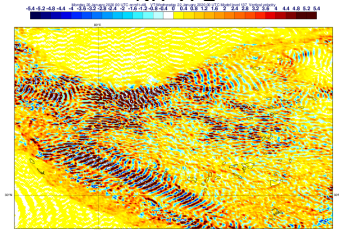
Remaining problem - Himalaya noise

Despite the fact that stability of time stepping was achieved still remaining sources of noise were present in the NH model simulations. w over Himalaya region, surface level 137.

HY VFE



NH VFE



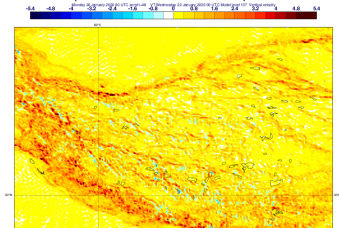
Noise removed with application of second order decentering of linear terms in ICI scheme.

$$\mathcal{L} \cdot \frac{X^{t+\delta t(0)} + X^t}{2}$$

replaced by

$$\mathcal{L} \cdot \frac{(1 + \epsilon)X^{t+\Delta t} + (1 - 2\epsilon)X^t + \epsilon X^{t-\Delta t}}{2}$$

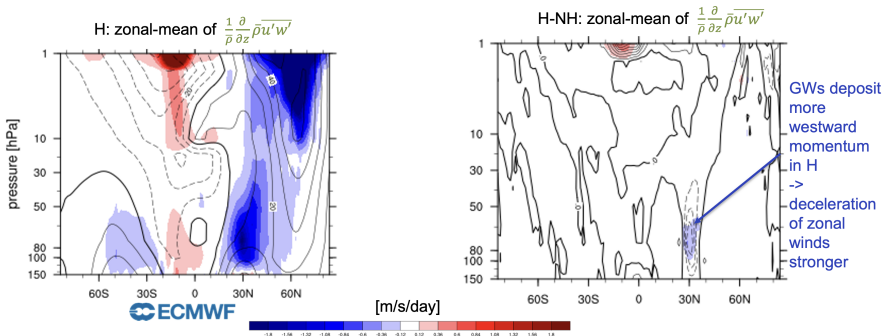
NH VFE + SIPR=850hPa + XIDT=0.14



Gravity waves - nonhydrostatic effects

H-IFS overestimates GW drag above the Himalayas in the subtropical jets. Zonal winds too weak in H-IFS.

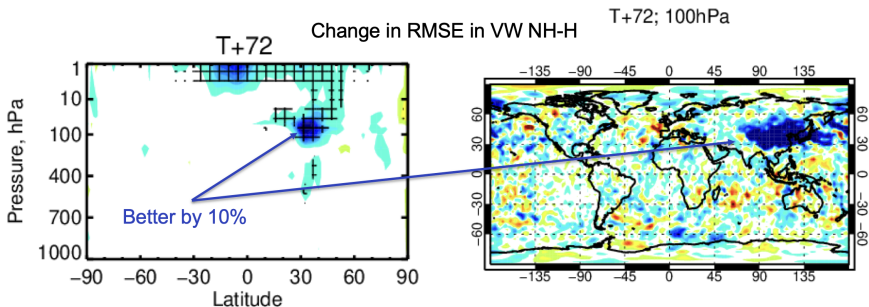
Example: 2.8 km resolution simulations for end of January 2022 (winds over Himalayas 50 m/s)



Gravity waves: Non-hydrostatic model impact on scores

Hydrostatic model overestimates GW drag above the Himalayas in the subtropical jets \Rightarrow Zonal winds too weaker in H-IFS.

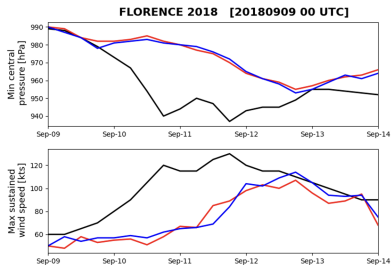
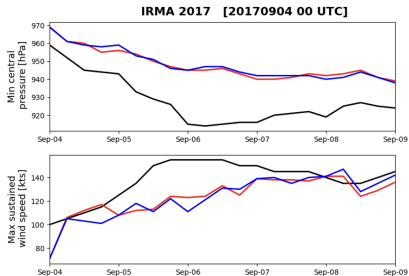
\Rightarrow Scores in vector winds 10% better in NH in Jan-Feb, in the lower stratosphere at 4.4km resolution. But NH-IFS is $> 2.5x$ more expensive than operational model.



Tropical cyclones (TC) - NH effects

Convection plays a big part in TC dynamics: Convective vertical velocities will be non-hydrostatic at small horizontal scales.

Q: Do NH effects matter for TC forecasts at 2.8km resolution? NO.



- New "D" spectral solver provided by ACCORD community was implemented into IFS,
- noise that appears in NH simulations for resolutions up to tco3999 was fixed by reformulation of VFE scheme, application of second order decentering and fix of spectral solver (single precision),
- stability at tco7999 was achieved by redefinition of vertical coordinate functions $A(\eta)$ and $B(\eta)$,
- clean intercomparison of NH and HY dynamics is ongoing (as NH simulation will provide exactly the same solution as HY dynamics when NH effects are negligible).
- NH-effects emerge for GWs for grid-spacings 4.4km, BUT only for very specific flow conditions and do not justify $> 2.5\times$ cost increase. No impact on TCs (or other investigated features) at 2.8km grid-spacing.